

Anderson localization of elementary excitations in a one dimensional Bose-Einstein condensate

N. Bilas and N. Pavloff

Laboratoire de Physique Théorique et Modèles Statistiques, Université Paris Sud, bât. 100, F-91405 Orsay Cedex, France

Received: date / Revised version: date

Abstract. We study the elementary excitations of a transversely confined Bose-Einstein condensate in presence of a weak axial random potential. We determine the localization length (i) in the hydrodynamical low energy regime, for a domain of linear densities ranging from the Tonks-Girardeau to the transverse Thomas-Fermi regime, in the case of a white noise potential and (ii) for all the range of energies, in the “one-dimensional mean field regime”, in the case where the randomness is induced by a series of randomly placed point-like impurities. We discuss our results in view of recent experiments in elongated BEC systems.

PACS. 03.75.Kk Dynamic properties of condensates; collective and hydrodynamic excitations, superfluid flow – 05.60.Gg Quantum transport

1 Introduction

The rapid developments of coherent atom manipulation which has recently allowed to study atomic interferometry of Bose-Einstein condensate (BEC) on a chip [1,2] opens up the prospect of considering a whole set of new transport phenomena in BEC systems. This can be considered as a new domain for studying the concepts issued from mesoscopic physics. As for the clean 2D electronic devices considered in this latter field, the BECs are genuinely phase coherent. Moreover, whereas interactions are difficult to model in mesoscopic physics, their effects in BEC systems are rather well understood and are expected to lead to a whole body of interesting phenomena: atom blockade [3], perfect solitonic-like transmission over a barrier [4], non linear resonant transport [5], breakdown and revival of Bloch oscillations [6], to mention just a few examples.

Coherent transport phenomena are of special interest in presence of disorder. Interference effects have then a prominent role, resulting, in the non interacting case, in weak or strong localization, as observed in many different fields (electronic or atomic physics, acoustics or electromagnetism). The influence of interaction on this phenomenon are of great interest (see, e.g., the review [7]) and have recently been addressed in the case of repulsive two body effective interaction for BEC systems in Refs. [8,9]. In these latter two references, interaction effects have been shown to lead to genuinely non-linear phenomena that profoundly alter the usual picture of Anderson localization.

In the present work, we also consider the influence of interaction on Anderson localization, but remaining at a

linear level, by studying the propagation of elementary excitations in a disordered BEC system. These are small deformations of a static background and they can be –at leading order– described in a linear framework (neglecting phenomena such as Beliaev damping). Interaction has nonetheless a prominent effect on the spectrum of elementary excitations, which is phonon-like at small energy and becomes similar to the one of non interacting particles at high energy. The crossover between these two regimes occurs at an energy $\hbar\omega$ of order of the chemical potential μ of the system.

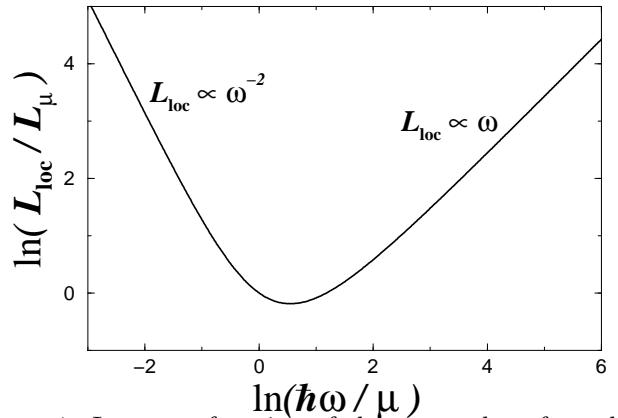


Figure 1: L_{loc} as a function of the energy $\hbar\omega$ of an elementary excitation in logarithmic scale (μ is the chemical potential of the system, and L_μ is the value of L_{loc} when $\hbar\omega = \mu$). The curve has been drawn within the model used in Section 4, employing formulas (40) and (61). This yields $\lambda^2 n_{imp} L_{loc} = 4[(\hbar\omega/\mu)^2 + 1]/[\sqrt{(\hbar\omega/\mu)^2 + 1} - 1]$ (the meaning of the parameters λ and n_{imp} in this formula is explained in Section 4).

Accordingly, the localization length L_{loc} of the elementary excitations (i.e., the typical extend of a localized mode, see Section 2 below) is expected to be similar to the one of phonons at low energy ($\hbar\omega \ll \mu$), and to the one of non interacting particles at high energy ($\hbar\omega \gg \mu$) [10]. The localization length of non interacting particles scales linearly with the energy (at high enough energy, see, e.g., [11]), whereas phonons in 1D disordered system have a localization length which diverges as ω^{-2} at small ω , as typically observed in models of disordered harmonic chains [12], in random layered media [13], or in continuous models with random elastic properties [14]. Hence, the localization length L_{loc} of the elementary excitations has the behavior illustrated in Figure 1, with a minimum at $\hbar\omega \simeq \mu$. The main purpose of the present work is to explicitly derive this type of behavior within several approximation schemes and different models of disorder.

The paper is organized as follows. In Section 2 we briefly present the model and the parameter range in which we are working, together with the Bogoliubov-de Gennes equations governing the dynamics of the elementary excitations. In Section 3 we consider the large wave-length limit within an hydrodynamical approach. We consider a Gaussian white noise potential and show in particular that in this domain, one obtains a ω^{-2} behavior of L_{loc} . In Section 4 we consider an other type of disorder (randomly placed delta impurities) and work within the transfer matrix approach. In this regime we are able to work for all the range of energies and obtain an analytic expression for L_{loc} in the scarce impurities limit. This expression matches at low energy the one obtained in Section 3 within the hydrodynamical approach. Very interesting recent experiments have addressed the issue of transport in a disordered BEC [15,16,17] and in Section 5 we discuss the relevance of our approach for analyzing some of the experimental results. Finally, some technical points are given in the Appendices. Appendix A is devoted to the derivation of a formula allowing to determine the density of state within the ‘‘phase formalism’’ employed in Section 3. In Appendix B we compute the transmission coefficient of an elementary excitation of energy $\hbar\omega$ over a single delta-like impurity.

2 The model

In this Section we present the basic equations describing the elementary excitations of a one dimensional (1D) Bose-Einstein condensed gas in presence of disorder. The condensate is formed by atoms of mass m which interact *via* a two-body potential characterized by its 3D s-wave scattering length $a > 0$. The gas is confined to one dimension by a transverse parabolic potential of frequency ω_{\perp} and ‘‘oscillator length’’ $a_{\perp} = (\hbar/m\omega_{\perp})^{1/2}$. There is no confinement in the axial (x) direction, but disorder is induced along the axis of the guide through a random potential $U(x)$ whose properties will be specified in the next sections.

In this Section (and also in Section 4) we restrict ourselves to the ‘‘1D mean field regime’’ [18] corresponding

to a density range such that

$$(a/a_{\perp})^2 \ll n_{\text{1D}} a \ll 1, \quad (1)$$

where n_{1D} denotes a typical order of magnitude of the 1D density $n(x, t)$ of the system. The first of the inequalities (1) ensures that the system does not get in the Tonks-Girardeau limit and the second that the transverse wave function is the ground state of the linear transverse Hamiltonian, see, e.g., the discussion in Refs. [18,19]. We address the low density case (Tonks-Girardeau limit) and the high density case (transverse Thomas-Fermi) in Section 3.

In the 1D mean field regime, the field operator is a function $\hat{\Psi}(x, t)$ which can be decomposed in the usual Bogoliubov way in c-number (the superfluid order parameter) plus small terms describing the contribution of the elementary oscillations (see, e.g., Ref. [20], chap. 5). For a stationary condensate, the order parameter is of the form $\psi(x) \exp\{-i\mu t/\hbar\}$ where $\psi(x)$ is real, and the Bogoliubov decomposition reads

$$\hat{\Psi}(x, t) = e^{-i\mu t/\hbar} \left\{ \psi(x) + \sum_{\nu} [u_{\nu}(x) \hat{b}_{\nu} e^{-i\omega_{\nu} t} + v_{\nu}^*(x) \hat{b}_{\nu}^{\dagger} e^{i\omega_{\nu} t}] \right\}, \quad (2)$$

where \hat{b}_{ν} and \hat{b}_{ν}^{\dagger} are, respectively, the annihilation and creation operator of the ν th elementary excitation. In the following, we drop the subscript ν for legibility. The order parameter verifies the Gross-Pitaevskii equation

$$-\frac{\hbar^2}{2m} \frac{d^2\psi}{dx^2} + \left\{ U(x) + g_{\text{1D}} \psi^2(x) \right\} \psi(x) = \mu \psi(x), \quad (3)$$

with $g_{\text{1D}} = 2\hbar\omega_{\perp} a$ [21,22,23]. The functions $u(x)$ and $v(x)$ are solutions of the Bogoliubov-de Gennes equations (see, e.g., Ref. [20], chap. 5)

$$\begin{pmatrix} H & g_{\text{1D}} \psi^2 \\ -g_{\text{1D}} \psi^2 & -H \end{pmatrix} \begin{pmatrix} u \\ v \end{pmatrix} = \hbar\omega \begin{pmatrix} u \\ v \end{pmatrix}, \quad (4)$$

where

$$H = -\frac{\hbar^2}{2m} \frac{d^2}{dx^2} + U(x) + 2g_{\text{1D}} \psi^2(x) - \mu. \quad (5)$$

In presence of a single elementary excitation of pulsation ω the density reads $n(x, t) = |\psi(x)|^2 + \delta n(x, t)$ where the density oscillation is, at leading order:

$$\delta n(x, t) = \psi(x)[u(x) + v(x)] e^{-i\omega t} + \text{c.c.}, \quad (6)$$

where ‘‘c.c.’’ stands for ‘‘complex conjugate’’. In Section 3 we use the notation $\delta n(x)$ for the quantity $\psi(x)[u(x) + v(x)]$.

In the absence of potential U , the order parameter is a constant $\psi(x) = n_0^{1/2}$ with $\mu = g_{\text{1D}} n_0$, the speed of sound in the system is $c_0 = (\mu/m)^{1/2}$ and the healing length is $\xi = \hbar/(m c_0)$.

Disorder is induced along the axis x of the guide through the random potential $U(x)$. Denoting U_{typ} the typical

value of $|U(x)|$, we work in the limit $U_{\text{typ}} \ll \mu$. This regime is easily reached experimentally [15,16] and is very relevant for our purpose because it corresponds to a range of parameters where Anderson localization is not blurred by effects connected to “fragmentation of the condensate” [24].

In a 1D disordered system the excitations are expected to be localized around a point with an envelop decreasing exponentially with the distance to this point. This corresponds to functions u , v and δn behaving as $\exp\{\pm\gamma x\}$ when $|x| \rightarrow \infty$. γ is a function of ω known as the Lyapunov exponent; it characterizes the localization properties of the system. Its inverse $L_{\text{loc}} = \gamma^{-1}$ is the localization length [11]. We determine the Lyapunov exponent of the system in Section 3 in the hydrodynamical regime $\hbar\omega \ll \mu$.

In Section 4 we approach the problem in a different –but equivalent– manner. The disordered potential is assumed to be non zero only in a finite region of space, between $x = 0$ and L . We consider an elementary excitation of pulsation ω incident on the random potential. The corresponding transmission coefficient T through the disordered region is related to the Lyapunov exponent *via* $\gamma = -\frac{1}{2} \lim_{L \rightarrow \infty} L^{-1} \ln T$ [11]. This is simply connected to the fact that the incident wave function decreases exponentially –at a rate γ – in the disordered region, and this corresponds finally to a transmission probability which is (within logarithmic accuracy) $T \sim \exp(-2\gamma L)$.

We note here important features of the localization properties of the elementary excitations. First, Eq. (4) admits a zero energy solution for $u(x) = -v^*(x) = \psi(x)$. Thus, whatever the disordered potential $U(x)$, the excitation at $\omega = 0$ is delocalized since $\psi(x)$ extends to infinity. This implies that L_{loc} diverges as $\omega \rightarrow 0$. Secondly, at $\omega \rightarrow \infty$ the high energy part of the spectrum is well described by a single particle description obtained by neglecting the coupling between the positive (u) and negative (v) frequency components of the excitations (see, e.g., Ref. [20], chap. 12). In this limit one can set $v = 0$ in Eq. (4) and the system is described by the Schrödinger-like Hamiltonian H (5) which localization length behaves as $L_{\text{loc}} \propto \omega$ at high energy. Thus, as already anticipated in the introduction, we expect a behavior of L_{loc} similar to what has been drawn in Fig. 1.

3 Hydrodynamical approach: $\hbar\omega \ll \mu$

The results obtained in this Section are derived within the 1D mean field regime (1). As explained at the end of the Section, they can be easily generalized in the transverse Thomas-Fermi regime and even in the Tonks-Girardeau limit.

In the present Section we only consider the low frequency excitations ($\hbar\omega \ll \mu$). These involve large wave lengths (which are of order $2\pi c_0/\omega$, when $\omega \rightarrow 0$) and accordingly, features at small length scale are not relevant in the potential seen by the excitations. In particular, the ground state order parameter can be evaluated in the

Thomas-Fermi approximation [25] leading to

$$\psi(x) = \sqrt{\frac{\mu - U(x)}{g_{1D}}}. \quad (7)$$

By reintroducing this ansatz in Eq. (3), one can easily show (provided U_{typ} is small compared to μ) that the Thomas-Fermi result (7) is valid in the limit $\xi \ll r_c$, where r_c fixes the length scale of typical variations of U (for instance this is the correlation length of the random potential). If besides, one considers the limit $\xi \ll c_0/\omega$, the density oscillations $\delta n(x)$ obey the hydrodynamical equation [26,27]

$$-\omega^2 \delta n(x) = \frac{d}{dx} \left(c^2(x) \frac{d}{dx} \delta n(x) \right), \quad (8)$$

where $c(x) = \{[\mu - U(x)]/m\}^{1/2}$ is a local sound velocity.

Disorder is induced along the axis of the guide through the random potential $U(x)$ which is assumed to have zero mean. The case $\langle U \rangle \neq 0$ can be treated with a trivial extension of the present approach which is explained at the end of the Section. In the following of this Section, U will be approximated by a Gaussian white noise. The hypothesis of white noise is only valid if the wave length of the excitations is large compared to the correlation length r_c of the true U (which is not a perfect white noise if we want the Thomas Fermi approximation (7) to hold). Hence, in the present Section, we make the consistent hypothesis that

$$\xi \ll r_c \ll \frac{2\pi c_0}{\omega}. \quad (9)$$

When the inequality (9) is verified, Equations (7) and (8) are both valid and furthermore the approximation of the random potential by a white noise is sound. In the following we thus write

$$\langle U(x)U(0) \rangle = \left(\frac{\hbar^2}{m} \right)^2 D \delta(x). \quad (10)$$

We now evaluate the localization length corresponding to Eq. (8) by means of the phase formalism (see Ref. [11]). We consider a real solution of (8) and define the functions $\alpha(x)$ and $\beta(x)$ by

$$\alpha(x) = \frac{\delta n(x)}{\delta n^*}, \quad \beta(x) = -\frac{c^2(x)}{c_0 \omega} \frac{d\alpha}{dx}. \quad (11)$$

In (11) the quantity δn^* is a typical value of $\delta n(x)$ which is introduced for dimensional purpose, but plays no role in the following [since Eq. (8) is linear]. The functions α and β satisfy the following system of equations:

$$\frac{d\alpha}{dx} = -\frac{\omega}{c_0} [1 + \eta(x)] \beta(x), \quad \frac{d\beta}{dx} = \frac{\omega}{c_0} \alpha(x). \quad (12)$$

In the first of equations (12), the term $\eta(x)$ is equal to $U(x)/[\mu - U(x)]$. In all the following we assume that U_{typ} is much smaller than μ , and we write $\eta(x) \simeq U(x)/\mu$ [28].

It is convenient to parametrize the functions α and β in the form

$$\alpha(x) = r(x) \cos \theta(x), \quad \beta(x) = r(x) \sin \theta(x). \quad (13)$$

The functions $\theta(x)$ and $r(x)$ describe respectively the phase and the envelope of the density oscillations $\delta n(x)$ [and accordingly of $u(x)$ and of $v(x)$]. In particular, the Lyapunov exponent is defined by

$$\gamma(\omega) = \lim_{x \rightarrow \infty} \frac{\langle \ln r(x) \rangle}{x}. \quad (14)$$

It is convenient to introduce the quantity $z = \alpha/\beta$ because, owing to the equality

$$\ln r^2(x) = \frac{2\omega}{c_0} \int_0^x z(x') dx' + \ln \beta(0) - \ln \sin^2 \theta(x), \quad (15)$$

and to the fact that the probability density of $\sin \theta$ (and thus also that of $z = \cot \theta$) becomes stationary (i.e., x independent) at large x [11], one can write

$$\gamma = \frac{\omega}{c_0} \lim_{x \rightarrow \infty} x^{-1} \int_0^x \langle z(x') \rangle dx' = \frac{\omega}{c_0} \langle z \rangle_{\text{st}}, \quad (16)$$

where $\langle z \rangle_{\text{st}}$ is the mean value of z in the stationary regime. This quantity is determined as follows. From (12) one sees that z verifies the following stochastic differential equation

$$-\frac{c_0}{\omega} \frac{dz}{dx} = 1 + z^2 + \frac{U(x)}{\mu}. \quad (17)$$

Let $P(z; x) dz$ be the probability that $z(x)$ lies in the interval $z, z + dz$. From (17) and (10) P verifies the Fokker-Planck equation (see, e.g., [11,29])

$$\frac{\partial P}{\partial x} = \frac{\omega}{c_0} \frac{\partial}{\partial z} \left[(1 + z^2) P + \frac{\omega \delta}{2} \frac{\partial P}{\partial z} \right], \quad (18)$$

where $\delta = \xi^4 D/c_0$. The stationary regime corresponds to the case where $\partial_x P = 0$. In this case, writing $P = P_{\text{st}}(z)$, Eq. (18) yields

$$(1 + z^2) P_{\text{st}} + \frac{\omega \delta}{2} \frac{dP_{\text{st}}}{dz} = J_\omega, \quad (19)$$

where J_ω is an integration constant. The solution of (19) is

$$P_{\text{st}}(z) = \frac{2 J_\omega}{\omega \delta} \int_0^{+\infty} dt \exp \left\{ \frac{2}{\omega \delta} \left[-(1 + z^2)t + zt^2 - \frac{t^3}{3} \right] \right\}. \quad (20)$$

The value of J_ω is fixed by the normalization of P_{st} . One obtains

$$J_\omega^{-1} = \sqrt{\frac{2\pi}{\omega \delta}} \int_{\mathbb{R}} \exp \left[-\frac{12t^2 + t^6}{6\omega \delta} \right] dt. \quad (21)$$

Simple algebra allows to express the average $\langle z \rangle_{\text{st}} = \int_{\mathbb{R}} z P_{\text{st}}(z) dz$ under the following form:

$$\langle z \rangle_{\text{st}} = J_\omega \sqrt{\frac{\pi}{2\omega \delta}} \int_{\mathbb{R}} \exp \left[-\frac{12t^2 + t^6}{6\omega \delta} \right] t^2 dt. \quad (22)$$

We are primarily interested in this Section in the small frequency evaluation of the Lyapunov exponent, because Eq. (8) is expected to describe the elementary excitations only in the domain $\hbar\omega/\mu \ll 1$. An expansion of the integrals (21) and (22) in the limit $\omega \delta \rightarrow 0$ yields, after reinserting in (16):

$$\gamma = \frac{\xi^2 D}{8} \left(\frac{\hbar\omega}{\mu} \right)^2 \left[1 - \frac{15}{16} \left(\frac{\omega \delta}{2} \right)^2 + \dots \right]. \quad (23)$$

Although the high frequency limit is not expected to be relevant in the hydrodynamical regime, we note for completeness that when $\omega \delta \rightarrow \infty$ one obtains

$$\gamma = \frac{\omega}{c_0} \sqrt{\frac{3}{8\pi}} \Gamma\left(\frac{5}{6}\right) \left(\frac{\omega \delta}{\sqrt{6}} \right)^{1/3} \times \left[1 - \frac{\Gamma(\frac{5}{6})}{\sqrt{\pi}} \left(\frac{\sqrt{6}}{\omega \delta} \right)^{2/3} + \left(\frac{2\sqrt{\pi}}{3\Gamma(\frac{5}{6})} - \frac{2[\Gamma(\frac{5}{6})]^2}{\pi} \right) \left(\frac{\sqrt{6}}{\omega \delta} \right)^{4/3} + \dots \right]. \quad (24)$$

The exact value of γ – as determined numerically from Eqs. (16), (21) and (22) – is represented in Fig. 2 (solid line).

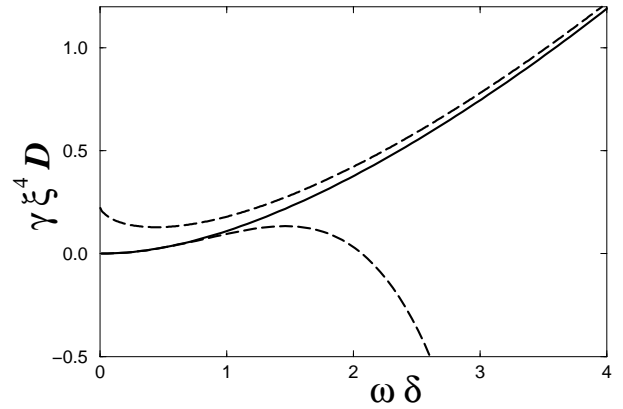


Figure 2: γ as a function of ω in rescaled units. The solid line is the numerical evaluation of γ using formulas (16) and (22). The dashed lines are the small and large $\omega \delta$ approximations [Eqs. (23) and (24)].

The quantity J_ω is also of interest for itself, because it gives informations on the density of states of the excitations. It is show in Appendix A that, if $N(\omega)$ denotes the integrated density of state per unit length, one has

$$N(\omega) = \frac{\omega}{c_0} J_\omega. \quad (25)$$

From (21) one gets the following expansions:

$$N(\omega) = \frac{3\omega}{c_0} \frac{\Gamma(\frac{5}{6})}{(2\pi)^{3/2}} \left(\frac{\omega\delta}{\sqrt{6}}\right)^{1/3} \times \left[1 + \frac{\Gamma(\frac{5}{6})}{\sqrt{\pi}} \left(\frac{\sqrt{6}}{\omega\delta}\right)^{2/3} + \dots \right], \quad (26)$$

when $\omega\delta \gg 1$, and

$$N(\omega) = \frac{\omega}{\pi c_0} \left[1 + \frac{5}{32} \left(\frac{\omega\delta}{2}\right)^2 + \dots \right], \quad (27)$$

when $\omega\delta \ll 1$. In the relevant regime of low excitation energies, the leading order in (27) coincides the result in absence of disorder, where one has a linear dispersion relation $\omega = c_0|q|$ in the hydrodynamical regime. This confirms what could have been already anticipated from the fact that $\gamma \rightarrow 0$ when $\omega \rightarrow 0$: the low lying excitations are poorly affected by the presence of disorder (the relevant small parameter being $\omega\delta$). In particular, there is no trapping of the elementary excitations by the disorder and no Lifshitz tail in the density of state. This is linked to the fact that $\omega = 0$ constitutes what is called a “stable genuine boundary of the spectrum” in the book by Lifshits, Gredeskul and Pastur (see Ref. [11], section 7.3).

The results presented in this Section have been obtained for a random potential with zero mean. They are very easily adapted to the case $\langle U \rangle \neq 0$: it suffices to write $U(x) = \langle U \rangle + U_1(x)$, and to define $\mu_1 = \mu - \langle U \rangle$, $c_1 = (\mu_1/m)^{1/2}$, $\xi_1 = \hbar/mc_1$, $\delta_1 = \xi_1^4 D/c_1$. Then, all the results presented from Eq. (11) to Eq. (27) remain valid provided $U(x)$, μ , c_0 , ξ and δ are replaced by the similar quantities with subscript “1”, with the coefficient D being now defined by $\langle U_1(x)U_1(0) \rangle = (\hbar^2/m)^2 D \delta(x)$ [instead of (10)].

The present hydrodynamical approach is very interesting because it has natural extensions out of the 1D mean field regime defined by Eq. (1). For high linear densities, when $n_{1D}a \gg 1$, one reaches the “transverse Thomas-Fermi regime” also named “3D cigar” in Ref. [18]. In this regime the system cannot be considered as truly unidimensional. However, the lowest branch of the spectrum corresponds to excitations that are isotropic in the transverse direction, and, as shown by Stringari in Ref. [30], they can still be described within the hydrodynamical approach. In this case, averaging the 3D hydrodynamical equation over the transverse direction, one gets a 1D equation of the form (8) where the local sound velocity $c(x)$ is now taken to be $c(x) = \{[\frac{1}{2}\mu - U(x)]/m\}^{1/2}$. So, all the results presented from Eq. (11) to Eq. (27) remain valid provided μ , c_0 and ξ and are replaced by $\mu' = \mu/2$, $c'_0 = (\mu'/m)^{1/2}$ and $\xi' = \hbar/(m c'_0)$.

The low density regime $n_{1D}a \ll (a/a_\perp)^2$ (Tonks-Girardeau) can also be studied within the hydrodynamical framework (see for instance Ref. [18]). In this case one has $\mu = (\pi \hbar n_0)^2/2m$, $c_0 = (2\mu/m)^{1/2}$ and Eq. (8) is replaced by

$$-\omega^2 \delta n(x) = \frac{d}{dx} \left\{ c(x) \frac{d}{dx} [c(x) \delta n(x)] \right\}, \quad (28)$$

with the local sound velocity being defined by $c(x) = \{[\frac{2}{m}[\mu - U(x)]]^{1/2}$. In the present case we define [instead of (11)]

$$\alpha(x) = \frac{c(x)}{c_0} \frac{\delta n(x)}{\delta n^*}, \quad \beta(x) = \frac{c(x)}{\omega} \frac{d\alpha}{dx}. \quad (29)$$

Writing $\alpha = r \sin \theta$ and $\beta = r \cos \theta$, one obtains:

$$\frac{dr}{dx} = 0, \quad \frac{d\theta}{dx} = \frac{\omega}{c(x)}. \quad (30)$$

From the second of these equations, in the limit where $1/c(x) = c_0^{-1}[1 + \frac{1}{2}U(x)/\mu]$, one can show that the phase $\theta(x)$ has a Gaussian distribution of the form

$$Q(\theta; x) = \frac{1}{\sqrt{2\pi\omega^2 x \delta / c_0}} \exp \left\{ -\frac{(\theta - \theta_0 - \frac{\omega x}{c_0})^2}{2\omega^2 x \delta / c_0} \right\}, \quad (31)$$

with $\delta = (\hbar^2/2m\mu)^2 D/c_0$.

The first of Eqs. (30) is more interesting. It shows that the envelope of function $\alpha(x)$ remains exactly constant. Assuming that the localization properties of $\alpha(x)$ are the same than those of $\delta n(x)$ [31], this equation points to the absence of exponential localization in the hydrodynamical limit of the Tonks-Girardeau regime.

4 Transfer Matrix approach

In this Section, we study Anderson localization of the elementary excitations of a Bose-Einstein condensate with an other type of disordered potential and in a framework different from the one used in the previous Section. Namely, we study the transmission through a disordered region of extend L , in the 1D mean field regime (1), by means of a transfer matrix approach for a disordered potential:

$$U(x) = g_{\text{imp}} \sum_n \delta(x - x_n), \quad \text{where} \quad g_{\text{imp}} = \lambda \mu \xi. \quad (32)$$

$U(x)$ describes a series of static impurities with equal intensity and random positions x_n . The peak intensity is measured by the dimensionless parameter λ . We consider here the repulsive case $\lambda > 0$. The x_n 's are uncorrelated and uniformly distributed with mean density n_{imp} . In this case $\langle U(x) \rangle = g_{\text{imp}} n_{\text{imp}}$ and $\langle U(x_1)U(x_2) \rangle - \langle U(x_1) \rangle \times \langle U(x_2) \rangle = (\hbar^2/m)^2 D \delta(x_1 - x_2)$, with $D = n_{\text{imp}} (\lambda/\xi)^2$. From what is known in the case of Schrödinger equation, this type of potential is typical insofar as localization properties are concerned [11]. Besides, it has recently been proposed to implement a very similar type of random potential by using two different atomic species in an optical lattice [32].

The static background is deformed around each impurity over a distance which is at most of order ξ . We consider the regime where this deformation does not extend to the nearest impurity ($n_{\text{imp}}\xi \ll 1$ [33]). In this case, the propagation of an elementary excitation in presence of the disordered potential $U(x)$ can be treated as

a sequence of scatterings over isolated perturbations. Besides –as shown in Appendix B– both the scattering of an elementary excitation over such a perturbation, and its propagation between two successive impurities (separated by a distance ℓ) are, in this regime, described by a 2×2 transfer matrix, denoted respectively \mathcal{T}_λ and $\mathcal{T}_0(\ell)$ with (see, e.g., [34])

$$\mathcal{T}_\lambda = \begin{pmatrix} 1/t_\lambda^* & -r_\lambda^*/t_\lambda^* \\ -r_\lambda/t_\lambda & 1/t_\lambda \end{pmatrix}, \quad \mathcal{T}_0(\ell) = \begin{pmatrix} 1/t_0^* & 0 \\ 0 & 1/t_0 \end{pmatrix}. \quad (33)$$

r_λ and t_λ in Eq. (33) are the transmission and reflexion amplitudes of an elementary excitation with energy $\hbar\omega$ across the background deformation induced by a single delta-like impurity. Their dependence on λ and ω is determined in Appendix B [Eqs. (57) and (58)]. The scattering states we choose for writing the matrices \mathcal{T}_λ and $\mathcal{T}_0(\ell)$ are the one introduced in this Appendix. They are pictured in Fig. 3.

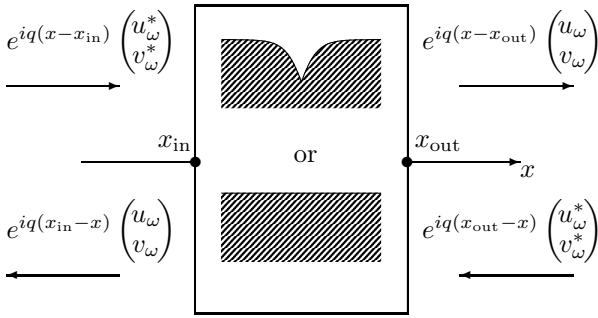


Figure 3: Scattering channels used for writing the transfer matrices \mathcal{T}_λ and $\mathcal{T}_0(\ell)$ of (33). In the case of unperturbed motion over a length ℓ one has $x_{\text{out}} - x_{\text{in}} = \ell$. In the case of scattering by a delta peak located at $(x_{\text{in}} + x_{\text{out}})/2$, one should take $\xi \ll x_{\text{out}} - x_{\text{in}} \ll n_{\text{imp}}^{-1}$.

The coefficients u_ω and v_ω in Figure 3 are chosen in order to make the incoming and outgoing channels identical to these appearing naturally in Appendix B when considering the scattering of an elementary excitation by a single impurity. One thus takes

$$\begin{pmatrix} u_\omega \\ v_\omega \end{pmatrix} = \begin{pmatrix} \left[\frac{q\xi}{2} + \frac{\omega}{c_0q} + i \right]^2 \\ \left[\frac{q\xi}{2} - \frac{\omega}{c_0q} + i \right]^2 \end{pmatrix}. \quad (34)$$

where q is defined in Eq. (56). In the case of scattering by an impurity, this corresponds indeed to the scattering channels defined by Eqs. (53), (54) and (55). In the case of free motion over a length ℓ , it is easy to see that these scattering channels correspond to a matrix $\mathcal{T}_0(\ell)$ such as defined in Eq. (33) with

$$t_0(\ell, \omega) = e^{i(q\ell - 2\alpha)}, \quad \text{where} \quad e^{-2i\alpha} = \frac{u_\omega^*}{u_\omega} = \frac{v_\omega^*}{v_\omega}. \quad (35)$$

Then, the scattering by a series of N delta peaks separated by distances $\ell_1 = x_2 - x_1, \dots, \ell_{N-1} = x_N - x_{N-1}$, is

described by the transfer matrix \mathcal{T}_N which is the product

$$\mathcal{T}_N = \mathcal{T}_\lambda \times \mathcal{T}_0(\ell_{N-1}) \times \mathcal{T}_\lambda \dots \times \mathcal{T}_0(\ell_1) \times \mathcal{T}_\lambda. \quad (36)$$

\mathcal{T}_N defined in Eq. (36) is of the general form

$$\mathcal{T}_N = \begin{pmatrix} 1/t_N^* & -r_N^*/t_N^* \\ -r_N/t_N & 1/t_N \end{pmatrix}. \quad (37)$$

Eq. (37) is used for computing the reflexion and transmission amplitudes (r_N and t_N) of the elementary excitation over the potential (32). The transmission probability over this potential is $T_N = |t_N|^2$.

As discussed at the end of Section 2, the analogous of the Lyapunov exponent already computed in Section 3 [Eq. (14)] is here defined as

$$\gamma = - \lim_{N \rightarrow \infty} \frac{n_{\text{imp}}}{N} \langle \ln |t_N| \rangle = - \lim_{N \rightarrow \infty} \frac{n_{\text{imp}}}{2N} \langle \ln T_N \rangle. \quad (38)$$

We calculated γ numerically, by a Monte Carlo averaging over 50 realizations of the disorder, taking $N = 2000$ [35]. The result is shown in Figure 4 for $\lambda = 1$ and $n_{\text{imp}}\xi = 0.02$. In the present model the lengths $\ell_i = x_{i+1} - x_i$ are independent, Poisson distributed, random variables with $P(\ell) = n_{\text{imp}} \exp\{-\ell n_{\text{imp}}\}$. Thus, for a fraction of lengths equal to $n_{\text{imp}}\xi$ the transfer matrix approach fails because the distance between two successive impurities is smaller than ξ [36]. This is the reason why we consider a rather small value of density of impurities: for the chosen value $n_{\text{imp}}\xi = 0.02$, only 2 % of the distances violate the criterion of applicability of the transfer matrix approach.

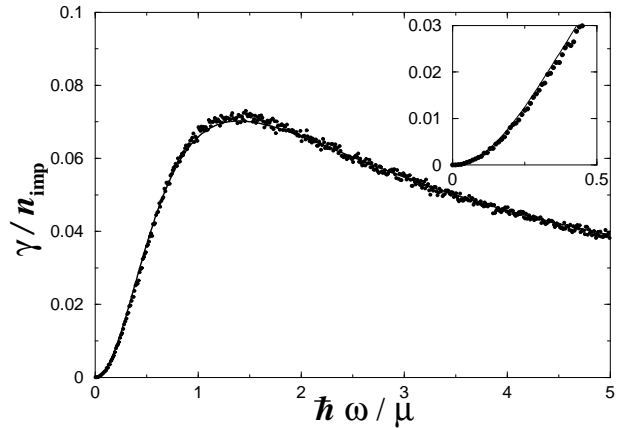


Figure 4: γ as a function of ω in rescaled units. The plot is drawn for $\lambda = 1$ and $\xi n_{\text{imp}} = 0.02$. The dots are the results of the numerical simulation and the solid line is the analytical result from Eq. (40). The inset displays a blowup of the figure at low energy.

As shown in Ref. [38], in the limit $n_{\text{imp}} \ll q$, one can obtain an analytical estimate of γ . From the relation $\mathcal{T}_{N+1} = \mathcal{T}_\lambda \times \mathcal{T}_0(\ell_N) \times \mathcal{T}_N$ one gets

$$\begin{aligned} \langle \ln |t_{N+1}| \rangle &= \ln |t_\lambda| + \langle \ln |t_N| \rangle \\ &- \left\langle \ln \left| 1 + r_\lambda r_N^* \frac{t_N}{t_N^*} t_0^2(\ell_N) \right| \right\rangle. \end{aligned} \quad (39)$$

ℓ_N is typically of order n_{imp}^{-1} , and in the limit $n_{\text{imp}} \ll q$, one may assume that the phase of $t_0(\ell_N, \omega)$ given in (35) is uniformly distributed in $[0, 2\pi]$. Then, the last term of the r.h.s. averages out to zero [37,38]. This yields

$$\gamma = -n_{\text{imp}} \ln |t_\lambda| = -\frac{n_{\text{imp}}}{2} \ln T_\lambda, \quad (40)$$

where we recall that the explicit expression of t_λ is given in Eq. (57) and $T_\lambda = |t_\lambda|^2$. Formula (40) corresponds to the solid line in Fig. 4. The agreement with the result of the numerical simulation is very good, even at low energy, as shown in the inset of the figure. This is not a surprise because the breakdown of (40) is expected only at extremely low energies for the present value n_{imp} : when $q \lesssim n_{\text{imp}}$, i.e., $\hbar\omega/\mu \simeq \xi q \lesssim 0.02$. For larger values of n_{imp} , the good agreement of Eq. (40) with the numerical data is limited to a smaller range of energies, mainly because the transfer matrix approach fails.

From Eq. (60), in the limit of small ω and $\lambda \ll 1$ formula (40) yields

$$\gamma \simeq \frac{\lambda^2}{8} \left(\frac{\hbar\omega}{\mu} \right)^2 n_{\text{imp}}. \quad (41)$$

The precise range of validity of formula (41) in the energy domain is expected to be $\xi n_{\text{imp}} \ll \hbar\omega/\mu \ll 1$; the first inequality ensures that (40) is valid and the second that (60) is applicable. The accuracy of formula (41) is tested in Fig. 5 in the case $\lambda = 0.2$ and $\xi n_{\text{imp}} = 0.03$. As already seen on Fig. 4, one notices on this Figure that the restriction $\xi n_{\text{imp}} \ll \hbar\omega/\mu$ turns out to be of no practical importance.

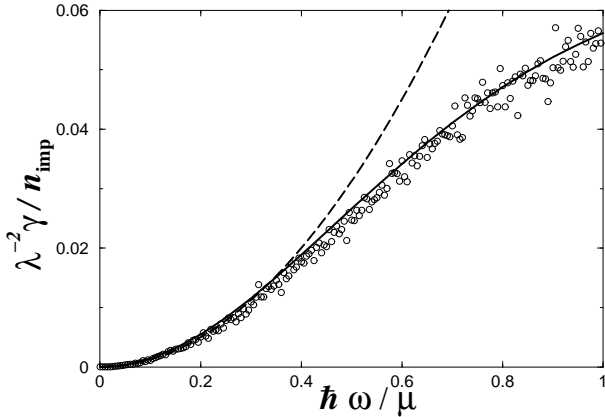


Figure 5: γ as a function of ω in rescaled units. The plot is drawn for $\lambda = 0.2$ and $\xi n_{\text{imp}} = 0.03$. The dots are the results of the numerical simulation and the solid line is the analytical result from Eq. (40). The dashed line is the approximate result (41).

Formula (41) is interesting because it is identical to the first term of expansion (23) which has been obtained in Section 3 in a completely different framework, and this permits to bridge the gap between the hydrodynamical approach and the present transfer matrix method. As just mentioned, formula (41) is restricted to small values of λ ,

but the approach of Section 3 is similarly limited to the domain $U_{\text{typ}} \ll \mu$. Also, Eq. (23) is restricted to small values of $\omega\delta$. But in the present case $\omega\delta = \xi n_{\text{imp}} \lambda^2 (\hbar\omega/\mu)$ is very small, even if $\hbar\omega \sim \mu$, so the restriction $\omega\delta \ll 1$ turns out to be of no practical importance here. Also, the results obtained in the present Section correspond to a potential with $\langle U \rangle = \lambda \mu \xi n_{\text{imp}} \neq 0$. However, the comparison with the results of Section 3 is possible with the rule given at the end of this Section for treating the case of a potential with non zero mean. In this case the first term of expansion (23) modifies to $\gamma = \frac{1}{8} \lambda^2 n_{\text{imp}} (\hbar\omega/\mu)^2 (1 - \lambda \xi n_{\text{imp}})^{-3}$. The correcting term $(1 - \lambda \xi n_{\text{imp}})^{-3}$, due to the non zero average of the potential, gives an undetectable modification of the result (the relative difference with (41) is of order 0.18 % in the case of Figure 5).

5 Discussion and conclusion

In this paper we have studied Anderson localization of elementary excitations in a 1D BEC system. Emphasis has been put on the determination of the localization length which has been determined in Section 3 using the “phase formalism” in the hydrodynamical approach (valid for $\hbar\omega \ll \mu$) and in Section 4, using a transfer matrix approach valid in the whole energy domain in the 1D mean field regime (provided $n_{\text{imp}} \xi \ll 1$). Results from the two approaches match within the appropriate limit. The hydrodynamic approach has the advantage of being able to deal with a large range of linear densities, ranging from the low density Tonks-Girardeau regime to the high density transverse Thomas-Fermi regime. In particular the puzzling absence of localization at low energy in the Tonks-Girardeau limit deserves further studies.

Our findings can be tested in realistic experimental setups. Up to now, 3 experiments, lead at Firenze, Orsay and Hannover, have been done which all use similar configurations [15,16,17]. Each of these experiments involves an elongated cigar shaped condensate in a magnetic trap with an optical speckle pattern creating the disordered potential [39]. The experimental random potential has a non zero mean value, and the experiments are done in the transverse Thomas-Fermi regime. We can thus study localization in this configuration using (for excitations of energy small compared to the chemical potential μ) the above hydrodynamical approach of Section 3 adapted as explained at the end of this Section (replacing in all the formulas μ by $\mu'_1 = \frac{\mu}{2} - \langle U \rangle$, $c'_1 = (\mu'_1/m)^{1/2}$, etc...). One writes $U(x) = \langle U \rangle + U_1(x)$. The auto-correlation $\langle U_1(x)U_1(0) \rangle$ has a typical range r_c which is in all the cases much larger than the healing length ξ : $r_c = 20 \mu\text{m}$ and $\xi = 0.35 \mu\text{m}$ in the Firenze experiment; $r_c = 5.2 \mu\text{m}$ and $\xi = 0.16 \mu\text{m}$ in the Orsay experiment [40]; $r_c \approx 7 \mu\text{m}$ and $\xi = 0.3 \mu\text{m}$ for $N = 8 \times 10^4$ atoms at Hannover. The condition (9) is fulfilled provided the pulsation ω of the excitations is much lower than $2\pi c'_1/r_c$ (which, for instance is equal to $2\pi \times 340 \text{ Hz}$ for $\langle U \rangle/\mu = 0.2$ in the Orsay experiment). In this regime, the potential can be approximated by a white noise with a coefficient D and a

correlation radius r_c defined by

$$\left(\frac{\hbar^2}{m}\right)^2 D = \int_{\mathbb{R}} \langle U_1(x)U_1(0) \rangle dx = \langle U \rangle^2 r_c. \quad (42)$$

Following the procedure explained in Section 3 this leads to

$$L_{loc} = \frac{\xi^2}{r_c} \left(\frac{\mu}{\langle U \rangle}\right)^2 \left(\frac{\mu}{\hbar\omega}\right)^2 \left(1 - \frac{2\langle U \rangle}{\mu}\right)^3. \quad (43)$$

The experimental configuration which is closer to the one considered in the present paper is the one of the Firenze group [15] which has studied elementary excitations of an elongated condensate in presence of a speckle pattern. The discrete excitation modes in elongated systems are similar to the continuous ones of infinite systems we have described in the present article only in the case of high quantum numbers (see, e.g., Ref. [20], chap. 12). Unfortunately, only the low lying dipole and quadrupole modes have been studied in Ref. [15]. We nonetheless discuss this experiment using our results, keeping in mind that we can only provide rough orders of magnitude.

The data of the Firenze group are presented in a way more easily analyzed within the model of random delta peaks of Section 4. However, in the regime where Eq. (43) is valid, all models are expected to yield the same result, as argued in Section 3 and verified in Section 4. The only relevant parameter being the parameter D , or equivalently r_c [which is related to D by (42)]. Within the model of random δ -peaks one has $\langle U \rangle = \lambda \mu \xi n_{imp}$ and $D = n_{imp}(\lambda/\xi)^2$ yielding $r_c = n_{imp}^{-1} = 20 \mu\text{m}$ [15]. The chemical potential in the Firenze experiment is $\mu = 1 \text{ kHz}$ and the excitations considered are the dipole ($\nu_1 = 8.74 \text{ Hz}$) and quadrupole ($\nu_2 = 13.8 \text{ Hz}$). For a disorder such that $\langle U \rangle/\mu = 0.1$ (which is typical in this experiment) the dipole excitation corresponds to a localization length $L_{loc}^1 = 4.1 \text{ mm}$, whereas for the quadrupole one gets $L_{loc}^2 = 1.6 \text{ mm}$ ($L_{loc}^2 = \frac{2}{5}L_{loc}^1$ since $\nu_2/\nu_1 = \sqrt{5/2}$). We also note that higher excited modes having frequency $\nu_n = \frac{\nu_1}{2} \sqrt{n(n+3)}$ [41,30] have lower localization lengths: $L_{loc}^n = \frac{4}{n(n+3)} L_{loc}^1$. L_{loc}^n becomes comparable with the typical axial size of the condensate ($110 \mu\text{m}$) for $n \sim 10$ [42].

A precise plot of the oscillations of a dipole mode is presented in Ref. [15] in the case $\langle U \rangle/\mu = 0.06$ which corresponds to a limit we can address using Eq. (43) [43]. An experimental estimate of the value of the localization length can be obtained by fitting the experimental data with a sinusoidal oscillation at frequency ν_1 with a damping $\exp\{-2X(t)/L_{loc}^{exp}\}$, where $X(t) = 4\Delta\nu_1 t$ is the distance traveled by the dipole mode for an oscillation of maximal amplitude Δ . From the data presented in Ref. [15] we obtain $L_{loc}^{exp} \simeq 1.7 \text{ mm}$. This does not agree with the value $L_{loc}^1 = 15 \text{ mm}$ obtained from Eq. (43) in the case $\langle U \rangle/\mu = 0.06$, but we recall that we do not expect the dipole mode to be equivalent to an excitation of an infinite system. Thus, the damping observed in the Firenze experiment [15] cannot be accounted for by a model of

infinitely long condensate with no axial trapping. Quantitative theoretical description of this experiment should take the axial trapping fully into account. We nonetheless hope that the experimental study of higher excited modes could directly confirm the result (43).

It is also interesting to discuss the expected localization length in the Orsay experiment [16], where the properties of the random potential are well characterized. In this experiment, the potential is Poisson distributed with a mean value $\langle U \rangle$ which is a fraction of the chemical potential ($\mu = 4.47 \text{ kHz}$). Taking $\langle U \rangle/\mu = 0.2$, and for instance $\omega = \omega_z = 2\pi \times 6.7 \text{ Hz}$ (corresponding to the dipole excitation) one obtains $L_{loc} = 11.8 \text{ mm}$. Besides, if one is able to generate excitations with $\omega \simeq 6 \times \omega_z$, one still remains in the hydrodynamical regime and the above value of L_{loc} is decreased by a factor 36, becoming of the order of the axial size of the condensate ($300 \mu\text{m}$ in the Orsay experiment [16]). We recall that the present approach does not strictly apply for low lying excitations of a trapped condensate, but it is nevertheless interesting to get an estimation of the typical length scale for observing Anderson localization experimentally.

We note that the Firenze [44], Orsay [16] and Hannover [17] groups observed a saturation of the expansion of a condensate in a disordered potential. In the 3 experiments this phenomenon has been interpreted (see also [45,46]) as being due to the trapping of the wings of the condensate by the large peaks of the speckle potential, with no relation to Anderson localization. We hope that in the near future, new experiments will be able to directly address Anderson localization of elementary excitations in transversely confined Bose-Einstein condensates, in configurations corresponding to the scenario analyzed in the present work. In this case, our study indicates that localization is more easily achieved for excitations of energy of order μ (see Fig. 1) created for instance through Bragg spectroscopy [47]. This range of energy is out of the hydrodynamical regime presented in Section 3, but the approach of Section 4 allows to get a quantitative estimate of L_{loc} in this case (for the 1D mean field regime).

It is a pleasure to acknowledge fruitful discussions with L. Pastur, G. Shlyapnikov and C. Texier. This work was supported by the Ministère de la Recherche (Grant ACI Nanoscience 201), by the ANR (grants ANR-05-Nano-008-02 and ANR-NT05-2-42103) and by the IFRAF Institute. Laboratoire de Physique Théorique et Modèles Statistiques is Unité Mixte de Recherche de l'Université Paris XI et du CNRS, UMR 8626.

A Appendix: Density of state within the phase formalism

In this Appendix we briefly demonstrate Eq. (25) following a similar demonstration in Ref. [11]. We first demonstrate that the phase θ defined in (13) is a monotonic function of ω . This can be shown by introducing the auxiliary variable $y = -c_0 z/\omega$. Expressing (17) in terms of the variable y ,

differentiating with respect to ω and then integrating the resulting equation one gets

$$\frac{\partial y}{\partial \omega} = \frac{2\omega}{c_0^2} \int_0^x dx' y^2(x') \exp\left\{\frac{2\omega^2}{c_0^2} \int_{x'}^x y(x'') dx''\right\} > 0. \quad (44)$$

Thus $z = -\omega y/c_0$ is a decreasing function of ω , and θ is an increasing function of ω (since θ is a continuous function and $\partial z/\partial \theta = -1 - z^2$). θ verifies the equation

$$\frac{c_0}{\omega} \frac{d\theta}{dx} = 1 + \sin^2 \theta \frac{U(x)}{\mu}. \quad (45)$$

The fact that θ is an increasing function of ω immediately implies that the number of eigenmodes [solutions of (8) or equivalently of (12)] with pulsation between 0 and ω , verifying the boundary condition $\cot \theta(0) = \theta_0$ and $\cot \theta(L) = \theta_L$ coincides with the number of pulsations $\omega' \in [0, \omega]$ for which the accumulated phase $\theta(\omega', L)$ as determined by (45) with the initial condition $\theta(\omega', 0) = \theta_0$ verifies $\theta(\omega', L) = \theta_L + m\pi$. This number is equal to

$$E \left[\frac{\theta(\omega, L) - \theta(0, L)}{\pi} \right] = E \left[\frac{\theta(\omega, L) - \theta_0}{\pi} \right], \quad (46)$$

where $E(x)$ denotes the integer part of x . Passing to the limit $L \rightarrow \infty$ and allowing for the fact the number of states is a self averaging quantity one obtains

$$N(\omega) = \lim_{L \rightarrow \infty} \frac{\langle \theta(\omega, L) \rangle}{\pi L}. \quad (47)$$

But the number (46) is also seen to be the number of times where the variable θ equals zero modulo π in the interval $[0, L]$. This stems from the fact that $\theta(x)$ can change interval $[n\pi, (n+1)\pi]$ only toward a higher interval and cannot go backward to a lower interval, because, as seen from (45), $d\theta/dx|_{\theta=n\pi} = \omega/c_0 > 0$. One may thus write

$$N(\omega) = \lim_{L \rightarrow \infty} \frac{\omega}{c_0 L} \int_0^L dx Q^{\text{red}}(0; x), \quad (48)$$

where

$$Q^{\text{red}}(\theta; x) = \sum_{n \in \mathbb{Z}} \left\langle \delta(\theta(x) - n\pi - \theta) \right\rangle, \quad (49)$$

is the probability density for the reduced phase. Owing to the fact that Q^{red} reaches a stationary (i.e., x independent) distribution $Q_{\text{st}}^{\text{red}}(\theta)$, (48) yields

$$N(\omega) = \frac{\omega}{c_0} Q_{\text{st}}^{\text{red}}(0) = \frac{\omega}{c_0} \lim_{z \rightarrow \infty} (1 + z^2) P_{\text{st}}(z), \quad (50)$$

where the last equality follows from the relation $z = \cot \theta$. The explicit expression (20) of P_{st} evaluated at large z then yields the desired result (25).

B Appendix: Transmission through a single delta peak

In this Appendix we determine the transmission and reflexion amplitude of an elementary excitation of energy

$\hbar\omega$ incident from the left on a delta-like impurity located at $x = 0$. These coefficients have already been obtained by Kagan *et al.* in the case of a barrier of finite width [48]. In the present case the impurity interacts with the atoms forming the condensate via a potential $\lambda \mu \xi \delta(x)$ with $\lambda > 0$. The condensate is deformed near the impurity and the order parameter reads

$$\psi(x) = \tanh(|x/\xi| + a), \quad \text{with} \\ a = \frac{1}{2} \sinh^{-1} \left(\frac{2}{\lambda} \right). \quad (51)$$

This form of $\psi(x)$ corresponds to two portions of black solitons matched together at $x = 0$ in order to satisfy the condition $\xi [\psi'(0^+) - \psi'(0^-)] = 2\lambda \psi(0)$. Far from the impurity (at $x \rightarrow \pm\infty$), the background is not perturbed and an elementary excitation of energy $\hbar\omega$ has a wave vector q such that $\omega = c_0 q (1 + q^2 \xi^2/4)^{1/2}$, and is described by $(u(x), v(x)) = \exp(iqx)(u_\omega, v_\omega)$ where – by Eq. (4) – the constants u_ω and v_ω are related by

$$\left(\frac{\xi^2 q^2}{2} + 1 - \frac{\hbar\omega}{\mu} \right) u_\omega + v_\omega = 0. \quad (52)$$

The background is deformed near the impurity [as described by (51)], and in this region the form of the wave function of the elementary excitation is affected in a non trivial manner. However, one still has an analytical description of the excitations around the stationary profile (51) because the expression of the excitation around a soliton is known (it is given by the squared Jost functions of the inverse problem [49], see also Appendix A of Ref. [50]). Thus one can write the appropriate incoming, transmitted and reflected modes of the problem. It is important however to realize that the system has also evanescent modes localized around the impurity [48]. More specifically, the scattering process of an excitation of energy $\hbar\omega$ incident from $-\infty$ is described by

$$\Xi^{(-)}(x) = A_{\text{inc}} \Xi_q^*(-x) + A_{\text{ref}} \Xi_q(-x) + A_{\text{eva}}^{(-)} \Xi_{ip}(-x), \quad (53)$$

when $x < 0$, and

$$\Xi^{(+)}(x) = A_{\text{tra}} \Xi_q(x) + A_{\text{eva}}^{(+)} \Xi_{ip}(x), \quad (54)$$

when $x > 0$. The indexes “inc”, “ref”, “tra” and “eva” correspond respectively to incident, reflected, transmitted and evanescent channels. The expression of $\Xi_k(x)$ ($k = q$ or ip) in (53) and (54) is

$$\Xi_k(x) = e^{ikx} \left(\begin{array}{l} \left[\frac{k\xi}{2} + \frac{\omega}{c_0 k} + i \tanh\left(\frac{x}{\xi} + a\right) \right]^2 \\ \left[\frac{k\xi}{2} - \frac{\omega}{c_0 k} + i \tanh\left(\frac{x}{\xi} + a\right) \right]^2 \end{array} \right), \quad (55)$$

and the quantities q and p are wave vectors related to ω by

$$q\xi = \sqrt{2} \left\{ \sqrt{(\hbar\omega/\mu)^2 + 1} - 1 \right\}^{1/2}, \\ p\xi = \sqrt{2} \left\{ \sqrt{(\hbar\omega/\mu)^2 + 1} + 1 \right\}^{1/2}. \quad (56)$$

The wave functions defined in Eqs. (53) and (54) are the most general solutions of (4) corresponding to an elementary excitation of energy $\hbar\omega$ incoming from the left and scattering on a potential $U(x) = \lambda \xi \mu \delta(x)$. In particular, the incident, transmitted and reflected components of (53,54) all verify (52) far from the impurity. The assumption $n_{\text{imp}}\xi \ll 1$ made in Section 4 ensures that the evanescent mode Ξ_{ip} does not reach the nearest impurity [51]. This is the reason why the scattering on potential (32) can be described via a transfer matrix approach using only 2×2 matrices.

The matching at $x = 0$ corresponds to $\Xi^{(-)}(0) = \Xi^{(+)}(0)$ and $d\Xi^{(+)}(x)/dx|_0 - d\Xi^{(-)}(x)/dx|_0 = 2\lambda\xi^{-1}\Xi(0)$. This yields a system of 4 linear equations determining the coefficients A_{ref} , A_{tra} , $A_{\text{eva}}^{(-)}$ and $A_{\text{eva}}^{(+)}$ in terms of A_{inc} . A tedious but straightforward computation yields

$$t_\lambda = \frac{A_{\text{tra}}}{A_{\text{inc}}} = \frac{1}{2} \left[\frac{2 + iq\xi \tanh(2a)}{-2 + iq\xi \tanh(2a)} + \frac{\Delta^*}{\Delta} \right], \quad (57)$$

and

$$r_\lambda = \frac{A_{\text{ref}}}{A_{\text{inc}}} = \frac{1}{2} \left[\frac{2 + iq\xi \tanh(2a)}{-2 + iq\xi \tanh(2a)} - \frac{\Delta^*}{\Delta} \right], \quad (58)$$

where

$$\Delta = 4 \left(\frac{\hbar\omega}{\mu} + 2i \tanh^2 a \right) \sqrt{\left(\frac{\hbar\omega}{\mu} \right)^2 + 1} + 2\xi(p + iq) \tanh a \left[\frac{2\hbar\omega}{\mu} + i(1 + \tanh^2 a) \right]. \quad (59)$$

The transmission probability $T_\lambda = |t_\lambda|^2$ has the asymptotic form $T_\lambda \simeq 1 - \lambda^2\mu/(2\hbar\omega)$ when $\omega \rightarrow \infty$, and in the opposite small energy limit ($\hbar\omega \ll \mu$) one has

$$T_\lambda \simeq 1 - \left(\frac{\hbar\omega}{2\mu} \right)^2 \left[1 - \frac{2}{\tanh a} + \tanh(2a) \right]^2 \underset{\lambda \rightarrow 0}{\simeq} 1 - \left(\frac{\lambda \hbar\omega}{2\mu} \right)^2. \quad (60)$$

A typical behavior of T_λ as a function of ω is plotted in Fig. 6. The transmission probability is 1 at small frequency. This anomalous behavior of the transmission at small energy has already been noticed in Ref. [48] in the case of a barrier of finite extend. It is also in agreement with the findings of Ref. [50] where a dark soliton with velocity $v_{\text{sol}} \rightarrow c_0$ (and thus reaching the limit where it becomes a mere density perturbation, i.e., a phonon, which is an elementary excitation with $q \rightarrow 0$) was shown to pass over an obstacle without radiating energy, i.e., without reflection.

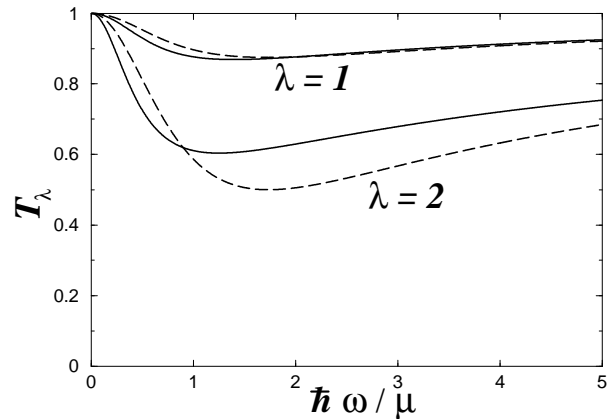


Figure 6: Transmission probability T_λ across a potential $U(x) = \lambda \mu \xi \delta(x)$ as a function of ω (in rescaled units). The solid line is the exact result (57) in the cases $\lambda = 1$ and $\lambda = 2$. The dashed line are the corresponding small λ approximations (61).

The exact formula for T_λ [from (57)] is compared on Figure 6 with an approximation valid for all ω when $\lambda \ll 1$:

$$T_\lambda \simeq 1 - \frac{(\lambda \xi q/2)^2}{(\hbar\omega/\mu)^2 + 1}. \quad (61)$$

It is seen on the Figure that this approximation is reasonably accurate already when $\lambda = 1$. More precisely, for $\lambda = 1$, the relative error due to the use of Eq. (61) is lower than 3 % (the error is maximum around $\hbar\omega \simeq 0.7\mu$); for $\lambda = 0.5$, this errors is lower than 0.5 %.

References

1. Y.-J. Wang *et al.*, Phys. Rev. Lett. **94**, 090405 (2005).
2. Y. Shin *et al.*, Phys. Rev. A **72**, 021604(R) (2005).
3. I. Carusotto and G. C. La Rocca, Phys. Rev. Lett. **84**, 399 (2000); I. Carusotto, Phys. Rev. A **63**, 023610 (2001).
4. P. Leboeuf, N. Pavloff and S. Sinha, Phys. Rev. A **68**, 063608 (2003).
5. T. Paul, K. Richter, and P. Schlagheck, Phys. Rev. Lett. **94**, 020404 (2005).
6. D. Witthaut, M. Werder, S. Mossmann, and H. J. Korsch, Phys. Rev. E **71**, 036625 (2005).
7. S. A. Gredeskul and Y. S. Kivshar, Phys. Rep. **216**, 1 (1992).
8. N. Bilas and N. Pavloff, Phys. Rev. Lett. **95**, 130403 (2005).
9. T. Paul, P. Leboeuf, N. Pavloff, K. Richter and P. Schlagheck, Phys. Rev. A **72**, 063621 (2005).
10. To our knowledge, this was first pointed out by G. Shlyapnikov (private communication).
11. I. M. Lifshits, S. A. Gredeskul, and L. A. Pastur, *Introduction to the theory of disordered systems*, John Wiley (New-York 1988).
12. K. Ishii, Prog. Theor. Phys. Suppl. **53**, 77 (1973).
13. V. Baluni and J. Willemsen, Phys. Rev. A **85**, 3358 (1985).
14. P. Sheng, B. White, Z.-Q. Zhang, and G. Papanicolaou, Phys. Rev. B **34**, 4757 (1986).

15. J. E. Lye *et al.*, Phys. Rev. Lett. **95**, 070401 (2005).
16. D. Clément *et al.*, Phys. Rev. Lett. **95**, 170409 (2005).
17. T. Schulte *et al.*, Phys. Rev. Lett. **95**, 170411 (2005).
18. C. Menotti and S. Stringari, Phys. Rev. A **66**, 043610 (2002).
19. D. S. Petrov, D. M. Gangardt, and G. V. Shlyapnikov, J. Phys. IV France **116**, 5 (2004).
20. L. Pitaevskii and S. Stringari, *Bose-Einstein Condensation*, Clarendon Press (Oxford 2003).
21. M. Olshanii, Phys. Rev. Lett. **81**, 938 (1998).
22. A. D. Jackson, G. M. Kavoulakis, and C. J. Pethick, Phys. Rev. A **58**, 2417 (1998).
23. P. Leboeuf and N. Pavloff, Phys. Rev. A **64**, 033602 (2001).
24. J. Fortágh, H. Ott, S. Kraft, A. Günther, and C. Zimmermann, Phys. Rev. A **66**, 041604(R) (2002); A. E. Leanhardt *et al.*, Phys. Rev. Lett. **89**, 040401 (2002); J. Estève *et al.*, Phys. Rev. A **70**, 043629 (2004).
25. Note that this is an *axial* Thomas-Fermi approximation which is done when the *transverse* wave-function is far from the Thomas-Fermi regime. When the transverse component gets also in the Thomas-Fermi regime, Eq. (7) still holds, but the form of the sound velocity in (8) is modified (as discussed at the end of Section 3).
26. S. Stringari, Phys. Rev. Lett. **77**, 2360 (1996).
27. P. Öhberg *et al.*, Phys. Rev. A **56**, R3346 (1997).
28. A mathematically more rigorous presentation would be to have made no hypothesis on the type of randomness of $U(x)$ so far, and only at the present point to make the assumption –based on physical motivations– that $\langle \eta \rangle = 0$ and $\langle \eta(x)\eta(0) \rangle = \xi^4 D \delta(x)$ which is equivalent to (10) if $\eta(x) = U(x)/\mu$.
29. C. Itzykson and J. M. Drouffe, *Statistical field theory*, volume 2, Cambridge University Press (Cambridge 1989).
30. S. Stringari, Phys. Rev. A **58**, 2385 (1998).
31. This makes sense when the typical value U_{typ} of $|U(x)|$ is much smaller than μ , since in this case $c(x)/c_0 \simeq 1$, and from (29) $\alpha(x)$ is thus roughly similar to $\delta n(x)$.
32. U. Gavish and Y. Castin, Phys. Rev. Lett. **95**, 020401 (2005).
33. This condition is valid even when $\lambda \rightarrow \infty$. In this case, each impurity induces a deformation of the background which is a black soliton centered at the position of the impurity, with typical extend ξ . The nearest impurity is typically located at distance n_{imp}^{-1} and thus does not see the perturbation induced by its neighbor if $n_{\text{imp}}\xi \ll 1$.
34. J. B. Pendry, Adv. Physics **43**, 461 (1994).
35. Since, $\ln |t_N|^2$ is a self averaging quantity, one could equivalently consider a single realization of the disorder with $N = 50 \times 2000$, see, e.g., A. Crisanti, G. Paladin, and, A. Vulpiani, *Products of Random Matrices*, Springer Series in Solid State Sciences **104**, Springer-Verlag (Berlin 1993).
36. The exact fraction of lengths inferior to ξ is $\int_0^\xi P(\ell) d\ell = 1 - \exp\{-\xi n_{\text{imp}}\}$, which is approximatively equal to ξn_{imp} when $\xi n_{\text{imp}} \ll 1$.
37. P. W. Anderson, D. J. Thouless, E. Abrahams, and D. S. Fisher, Phys. Rev. B **22**, 3519 (1980).
38. M. V. Berry and S. Klein, Eur. J. Phys. **18**, 222 (1997).
39. The Hannover experiment has the possibility of an additional optical lattice.
40. The conventions we use in the present work is slightly different from the ones of Ref. [16] : we note r_c what is denoted by Δz in this reference, and there is a difference by a factor $\sqrt{2}$ in our definition of ξ and in the one used in Ref. [16].
41. M. Fliesser, A. Csordás, P. Szépfalussy, and R. Graham, Phys. Rev. A **56**, R2533 (1997).
42. A possible way to further decrease the localization length would be to decrease the typical peak spacing of the speckle pattern.
43. The damping of the dipole oscillations are also studied for other amplitude of disorder in Ref. [15]: $\langle U \rangle / \mu = 0.4$ and 1, but we cannot address these regimes, Eq. (43) being only valid if $2 \langle U \rangle / \mu \ll 1$.
44. C. Fort *et al.*, Phys. Rev. Lett. **95**, 170410 (2005).
45. M. Modugno, Phys. Rev. A **73**, 013606 (2006).
46. L. Sanchez-Palencia *et al.*, private communication, in preparation.
47. S. Richard *et al.*, Phys. Rev. Lett. **91**, 010405 (2003).
48. Yu. Kagan, D. L. Kovrizhin, and L. A. Maksimov, Phys. Rev. Lett. **90**, 130402 (2003).
49. X.-J. Chen, Z-D Chen, and N.-N. Huang, J. Phys. A **31**, 6929 (1998).
50. N. Bilas and N. Pavloff, Phys. Rev. A **72**, 033618 (2005).
51. This is due to the exponential decrease $\exp\{-p|x|\}$ of these modes, and to the fact that, from (56), the wave vector p is approximatively $2\xi^{-1}$ when $\omega \rightarrow 0$, and $[2\omega/(\xi c_0)]^{1/2}$ when $\omega \rightarrow \infty$. Thus, $\exp\{-p/n_{\text{imp}}\}$ is always small.